Inorganic Chemistry

Article

pubs.acs.org/IC

New Metal-Only Lewis Pairs: Elucidating the Electronic Influence of *N*-Heterocyclic Carbenes and Phosphines on the Dative Pt-Al Bond

Jürgen Bauer, Rüdiger Bertermann, Holger Braunschweig,* Katrin Gruss, Florian Hupp, and Thomas Kramer

Institut für Anorganische Chemie, Julius-Maximilias-Universität Würzburg, Am Hubland, 97074 Würzburg, Germany

Supporting Information

ABSTRACT: The synthesis and full characterization of a new heteroleptic *N*-heterocyclic carbene (NHC)−phosphine platinum(0) complex and formation of its corresponding alane adduct is reported. The influence of the ligands on the Lewis basic properties was studied via multinuclear NMR-spectroscopy, X-ray analyses, and density functional theory (DFT) calculations. Consistently, the effect of changing the halogens upon the Lewis acid properties of aluminum halides was studied by X-ray analysis and DFT calculations.

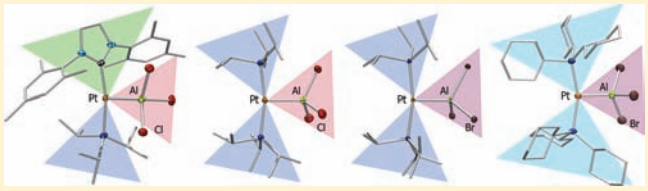

INTRODUCTION

Currently, the concept of metal-centered Lewis basicity is under intense investigation in organometallic research, and we are particularly interested in *unsupported* metal-only Lewis pairs (MOLPs). Lewis basic behavior of electron-rich transition metal complexes was observed in the early 1960s by the groups of Vaska and Wilkinson by means of rhodium and iridium species.[1,2] Subsequently, studies on the reactivity of *trans*-$[IrCl(CO)(PPh_3)_2]$ (**1**) toward protic substrates played a central role in the development of metal-centered Lewis basicity.[3] Early attempts to apply metal-centered nucleophilicity resulted in Lewis acid−base adducts of metals with small molecules, for example, BF_3,[4] although the proposed borane complexes were later refuted.[5] Nonetheless this work led to the development of metal-centered Lewis basicity as a synthetic concept in inorganic chemistry.[6] In the following years, half-sandwich compounds of the general formula $[CpL_nM]$ (M = Co, Rh, Ir) predominantly served as examples of metal-centered Lewis basicity. For instance, the group of Werner studied the Lewis basic properties of the complex $[Cp(Me_3P)_2Co]$ (**2**), which reacted with a variety of electrophiles (**3**−**5**).[7,8] Using analogous rhodium compounds, Mayer et al. examined half-sandwich adducts of the type $[Cp(R_3P)_2Rh{-}AlR'_3]$ (R = Me, Et; R′ = Me, Et) (**6**−**8**) by multinuclear NMR spectroscopy. Thereby, the Lewis acidic behavior of certain alanes toward transition metal Lewis bases was introduced, and kinetic and thermodynamic data were provided.[9] Additionally, $[Cp(Me_3P)Rh(Al_2Me_4Cl_2)]$ (**9**) could be studied by X-ray structural analysis. $[(Cp^*)(Me_3P)(H)_2Ir{-}AlPh_3]$ (**10**) (Cp* = 1,2,3,4,5-pentamethylcyclopentadienyl) was reported by Bergmann et al. as the first structurally characterized neutral transition metal aluminum complex. However, according to X-ray structural analysis the Ir−Al bond of **10** is supported by two H-atoms (Figure 1).[10] Additional density functional theory (DFT) calculations carried out by Lelj on this complex indicate a significant charge donation from the transition metal to the aluminum atom.[11] Descending the third row of the periodic table, Fischer delivered an example of a transition metal gallium adduct, the complex $[Cp^*(Cp^*Ga)_2Rh{-}GaCl_3]$ (**11**).[12]

The coordination chemistry of the lightest group 13 homologue, boron, has since been studied in a variety of different ligand classes, mainly three-coordinate boryl ligands, because of their essential roles in the transition metal-catalyzed hydroboration, diboration, and other boron addition reactions to unsaturated organics.[13−17] As is well-known, the reaction of electron rich late transition metal complexes with boron halides results in oxidative addition of a B−X bond.[18,19] This was consistently shown by our group using the complex $[(Cy_3P)_2Pt]$ (**12**), affording *trans*-(halo)(boryl) complexes.[20−23] Accordingly, in a recent DFT study Sakaki et al. proposed a possible mechanism for the oxidative addition of boranes to late transition metals.[24] The formation of the final *trans*-(bromo)(boryl) platinum(II) complex is enabled by coordination of the borane to platinum(0), resulting in a complex that can be considered as a Lewis acid−base adduct. In conclusion it seems that for Lewis acidic molecules with appropriate empty orbitals, oxidative addition may proceed by a prior M→E donation.[24] Similarly, the reaction of the heavier homologues $GaBr_3$ and GaI_3 with late transition metals results in oxidative addition products: *trans*-(halo)(gallyl) complexes.[25] In contrast, $GaCl_3$ follows a different reaction pathway, namely, the formation of an *unsupported* Lewis acid−base adduct.[25] Accordingly, Frenking et al. indicated, using DFT calculations on late transition metal adduct complexes with the general formula $[(Me_3P)_2M{-}EX_3]$ (M = group 10 metal; E = group 13 element; X = halogen), that M−E (E = Al, Ga) bond strength increases in the order F < Cl < Br < I, in agreement with the trends of Lewis acidity of boron halides and in the order F > Cl > Br > I for heavier group 13 halides.[26,27]

Received: November 22, 2011
Published: May 1, 2012

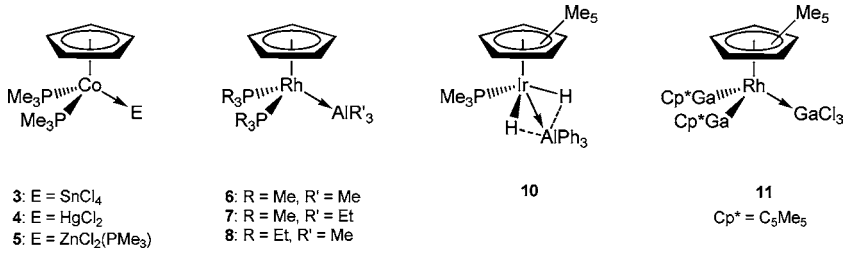

Figure 1. Metal-complexes **3**−**8**, **10**, **11**.

Herein we report the synthesis and full characterization of the new heteroleptic NHC−phosphine−Pt(0) complex [(IMes)(iPr$_3$P)Pt] (**13**) (IMes = *N*,*N*′-bis(2,4,6-trimethylphenyl)imidazol-2-ylidene). The reactivity toward AlX_3 was investigated, and the corresponding alane adducts [(IMes)(iPr$_3$P)Pt−AlX_3] (**14** X = Cl, **15** X = Br) were fully characterized. To the best of our knowledge, the complex [(IMes)(iPr$_3$P)Pt−$AlBr_3$] (**15**) is the first example of a heteroleptic phosphine/NHC platinum metal base with the Lewis acid $AlBr_3$. For structural and spectroscopic comparison the alane adducts [(iPr$_3$P)$_2$Pt−AlX_3] (**16**: X = Cl, **17**: X = Br) were synthesized. Aluminum chloride was employed in these studies as it is widely used as a strong Lewis acid.[28,29] The influence of NHC and R_3P ligands on the Lewis basicity of Pt(0) complexes was inferred on the basis of structural, spectroscopic, and computational data. For compounds **16** and **17**, both ^{27}Al NMR and ^{195}Pt NMR spectra were obtained, both of which displayed a $^1J(^{27}Al-^{195}Pt)$ spin−spin coupling—to the best of our knowledge the first time this coupling has been observed.

■ RESULTS AND DISCUSSION

Synthesis of NHC-Containing Pt(0) Complexes. To gain a better understanding of the dative bond between two metals, our group employed the well-established transition metal Lewis base [(Cy$_3$P)$_2$Pt] (**12**) to synthesize *unsupported* MOLPs containing the d-block metal platinum and representative Lewis acidic s-, p-, and d-block metal fragments. The reactions of the strong Lewis acids $BeCl_2$, $AlCl_3$, $GaCl_3$, and $ZrCl_4$ with **12** resulted in MOLPs of the general formula [(Cy$_3$P)$_2$Pt−ECl_n] (E = Be, Al, Ga, Zr, n = 2, 3, 4) (**18**−**21**) (Figure 2).[25−32] Hence, we were interested in varying, and

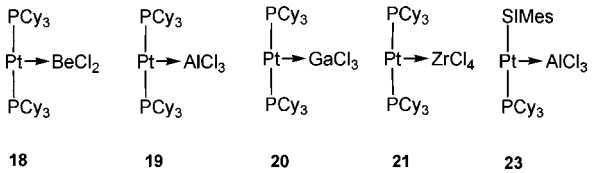

Figure 2. Metal-only-Lewis pairs **18**−**21** and **23**.

preferably increasing, the electron-donating properties of complexes of the type [L$_2$Pt] and thus prepared new heteroleptic 14-electron platinum(0) complexes and their corresponding $AlCl_3$ adducts using NHCs (*N*-heterocyclic carbenes), for example, [(SIMes)(Cy$_3$P)Pt] (**22**) and its alane adduct [(SIMes)(Cy$_3$P)Pt−$AlCl_3$] (**23**), respectively (SIMes = *N*,*N*′-bis(2,4,6-trimethylphenyl)imidazolylidene). Consequently, the direct influence of NHCs on the Lewis basic properties of the central metal was analyzed.[33]

In general, the influence of ligands can be varied in terms of their steric and electronic properties. An elegant method for quantification of the steric demand of various ligands is the "buried volume" method, developed recently by Nolan and Cavallo.[34,35] Alternatively, the analysis of the Tolman's electronic parameters (TEP) can be used for comparison of the electron-donor ability of the ligands.[36−38] A pioneering attempt to compare the steric and electronic properties of several alkyl and aryl phosphines was made by Tolman, comparing spectroscopic properties of transition metal phosphine complexes.[36] On a smaller scale, our group examined several platinum complexes by multinuclear NMR spectroscopic and X-ray structural analyses to verify the properties of PiPr$_3$ and PCy$_3$.[39−41] It was also found that the larger and more electron-donating the phosphine, the higher the catalyst activity in olefin metathesis.[42] In particular, PCy$_3$ turned out to be the ligand of choice in the famous "Grubbs 1st generation catalyst".[42] Several years later the substitution of one phosphine by one *N*-heterocyclic carbene led to a phosphine NHC complex with increased catalytic activity, the so-called "Grubbs 2nd generation catalyst".[43,44] Further attempts should be made to vary the ligand sphere of the complexes [L$_2$Pt] by reducing the steric demand of the PR$_3$ ligands. As shown below, PiPr$_3$ is the least σ-electron donating ligand of the mentioned ligands (Table 1). However, these measures of steric hindrance are not without controversy, as the $\%V_{bur}$ of PiPr$_3$ is greater than PCy$_3$, yet the cone angle is smaller.[45,46]

Table 1. TEP and $\%V_{bur}$ for PiPr$_3$, PCy$_3$, IMes, and SIMes

	PiPr$_3$	PCy$_3$	SIMes	IMes
TEP [cm^{-1}] (Ni(CO)$_3$L)	2059[a]	2056[a]	2052[b]	2050[b]
$\%V_{bur}$ (LAuCl)[c]	34.0[d]	33.4[d]	36.9[e]	36.5[e]
cone angle [deg][c]	160	170		

[a]Ref 34. [b]Ref 45. [c]Ref 46. [d]M−L = 2.28 Å. [e]M−L = 2.00 Å.

To vary the steric and electronic properties of homo- and heteroleptic platinum complexes, [(iPr$_3$P)$_2$Pt] (**24**) was used as starting material for the synthesis of the heteroleptic platinum(0) complex [(IMes)(iPr$_3$P)Pt] (**13**). To this end, **24** was stirred with a stoichiometric amount of IMes in a ligand-exchange reaction at ambient temperature in hexane. As **24** is obtained from the tris(phosphine) complex [(iPr$_3$P)$_3$Pt] (**25**) upon heating or in vacuo,[47,48] we also reacted **25** directly with equimolar amounts of IMes in hexane. Multinuclear NMR spectroscopy of the reaction mixture, as well as a color change from colorless to yellow, revealed complete consumption of the starting materials and formation of [(IMes)(iPr$_3$P)Pt] (**13**), which was isolated by crystallization from hexane at −30 °C in 60% yield.

Substitution of one phosphine by an NHC causes a slight high-field shift of the ^{31}P{^{1}H} NMR spectroscopic resonance of

13 to δ = 69.4 ppm (**24**: δ = 74.0 ppm). This is in accord with previous findings, particularly in case of the synthesis of [(SIMes)(Cy_3P)Pt] (**22**) (δ = 58.4 ppm, $^1J_{P-Pt}$ = 3640 Hz) from [($Cy_3P)_2$Pt] (**12**) (δ = 62.3 ppm, $^1J_{P-Pt}$ = 4160 Hz) by phosphine/carbene-exchange.[33] Additionally, the coupling constants are somewhat smaller (**13**: $^1J_{P-Pt}$ = 3897 Hz) compared to the starting material **24** ($^1J_{P-Pt}$ = 4104 Hz). These spectroscopic parameters (Table 2) are in line with recent findings, which indicate decreased Pt−P bond strengths as a result of the enhanced *trans*-influence of the NHC ligand.[33] The resonance of the carbenoid carbon atom in the $^{13}C\{^1H\}$ NMR spectrum of **13** (δ = 201.5 ppm) is in the expected range for late transition metal NHC complexes, such as [(IMes)$_2$Pt] (**26**) published by Arduengo et al. (δ = 197.5 ppm).[49] An additional measurement of the $^{195}Pt\{^1H\}$ NMR resonances revealed a slight downfield shift for compound **13** (δ = −6290 ppm) relative to its precursor complex **24** (δ = −6590 ppm). These findings are similar to the complex [(SIMes)(Cy_3P)Pt] (**22**) (δ = −6151 ppm) and its precursor complex [($Cy_3P)_2$Pt] (**12**) (δ = −6501 ppm). Overall, the spectroscopic similarities between **22** and **13** are obvious, indicating closely related compounds despite their different ligands.

Table 2. NMR Spectroscopic Parameters in Solution of Compounds 12−17, 19, 24, 27

	$^{31}P\{^1H\}^a$	$^1J_{P-Pt}{}^b$	$^{13}C\{^1H\}^{a,c}$	$^{195}Pt\{^1H\}^a$	$^{27}Al^a$	$^1J_{Al-Pt}{}^b$
12	62.3	4160		−6501		
19	53.5	3032		*d*	67.5	2034
13	69.4	3897	201.5	−6290		
14	56.9	2988	179.7	*d*	68.9	2100
15	53.5	2980	167.9	*d*	42.7	2200
16	65.5	3034		−5550	68.5	1933
17	63.1	3061		−5410	44.6	1999
24	74.0	4104		−6590		
27	51.2	3046		*d*	41.3	2150

[a] δ in ppm. [b] Coupling constants in Hz. [c] Signal of carbenoid carbon. [d] Not detected.

Light yellow crystals suitable for X-ray structure determination were obtained from a hexane solution at −30 °C. Complex **13** crystallizes in the space group $P\bar{1}$ and displays the expected overall linear geometry around the platinum center (Figure 3). A comparison with the above-mentioned complex **26** reveals comparable structural features, such as C−Pt−X angles (**13** (X = P): 175.71(7)°, **26** (X = C): 177.4(3)°) and Pt−C distances, respectively (**13**: 1.996(2) Å, **26**: 1.959(8) Å).

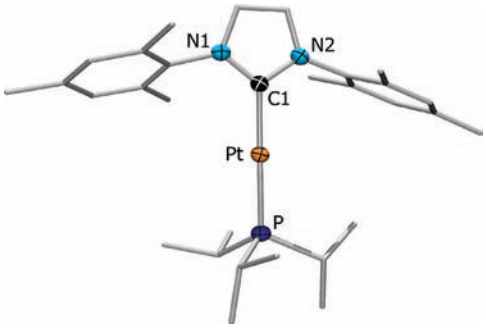

Figure 3. Molecular structure of **13**. Relevant bond lengths [Å] and angles [deg]: Pt−C1 1.996(2), Pt−P 2.208(1); C1−Pt−P 175.71(7). Ellipsoids are drawn at the 50% probability level. Ellipsoids of the ligands and hydrogen atoms are omitted for clarity.

To provide information on the propensity of the homoleptic bis(phosphine) complex **24** and the new heteroleptic species **13** to form MOLPs, we subsequently targeted the synthesis of the alane adducts [(IMes)(iPr_3P)Pt−AlX_3] (**14**: X = Cl, **15**: X = Br) and [($iPr_3P)_2$Pt−AlX_3] (**16**: X = Cl, **17**: X = Br), respectively.

Synthesis of Lewis Acid−Base Adducts. In analogy to previous results, the MOLPs **14**, **15** and **16**, **17** were synthesized by stirring the precursors **13** and **24** in benzene at ambient temperature with equimolar amounts of $AlCl_3$ or $AlBr_3$. These reactions yielded the expected T-shaped Lewis acid−base adducts [(IMes)(iPr_3P)Pt−AlX_3] (**14**: X = Cl, **15**: X = Br) and [($iPr_3P)_2$Pt−AlX_3] (**16**: X = Cl, **17**: X = Br) according to Scheme 1.

Scheme 1. Formation of the Complexes [(IMes)(iPr_3P)Pt−AlX_3] (14 = Cl, 15 = Br) and [($iPr_3P)_2$Pt−AlX_3] (16 = Cl, 17 = Br).

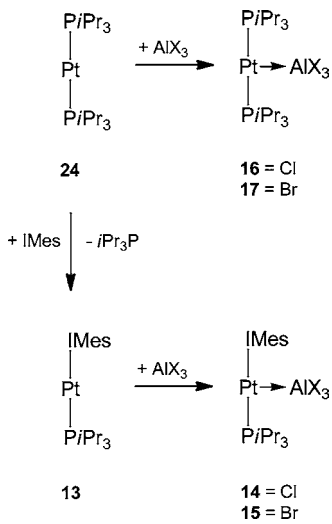

The formation of the MOLPs is confirmed by multinuclear NMR spectroscopy in solution. For the heteroleptic adduct **14** the $^{31}P\{^1H\}$ NMR spectrum reveals a singlet at δ = 56.9 ppm flanked by Pt satellites ($^1J_{P-Pt}$ = 2988 Hz), and for **15** the $^{31}P\{^1H\}$ NMR spectrum shows a signal at δ = 53.5 ppm ($^1J_{P-Pt}$ = 2980 Hz, while the bis(phosphine) adduct **16** shows a singlet at δ = 65.5 ppm ($^1J_{P-Pt}$ = 3034 Hz) and **17** shows a signal at δ = 63.1 ppm ($^1J_{P-Pt}$ = 3061 Hz). Altogether, the high-field shift of the $^{31}P\{^1H\}$ NMR resonances and the decrease of the $^1J_{P-Pt}$ coupling constants by about 1000 Hz in comparison to those of the precursors **13** (δ = 69.4 ppm, $^1J_{P-Pt}$ = 3897 Hz) and **24** (δ = 74.0 ppm, $^1J_{P-Pt}$ = 4104 Hz) is in good agreement with analogous systems, for example, [($Cy_3P)_2$Pt−$AlCl_3$] (**19**) (δ = 53.5 ppm, $^1J_{P-Pt}$ = 3032 Hz) and [($Cy_3P)_2$Pt−$AlBr_3$] (**27**) (δ = 51.2 ppm, $^1J_{P-Pt}$ = 3046 Hz).[31]

*$^{195}Pt\{^1H\}$ and ^{27}Al NMR Spectra of the Bisphosphine Adducts **16**, **17**, **19**, and **27**.* We were able to obtain relatively sharp $^{195}Pt\{^1H\}$ and ^{27}Al NMR spectra with well resolved spin−spin coupling information for the symmetrical bis(phosphine) compounds **16** and **17**. Although ^{27}Al with its high quadrupole moment is involved in the spin system, all couplings were observable, because of the axial symmetry of the complexes **16** and **17**, leading to a small electric field gradient

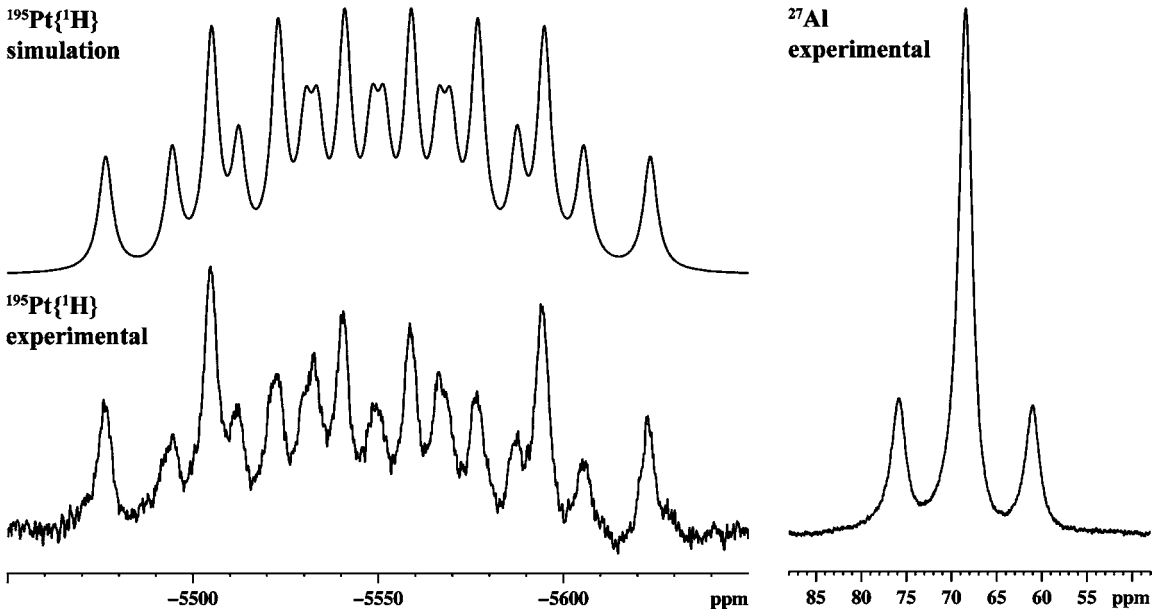

Figure 4. $^{195}Pt\{^1H\}$ NMR (left) and ^{27}Al NMR (right) spectra of **16**. The experimental $^{195}Pt\{^1H\}$ NMR spectrum (left, bottom) was recorded at 107.5 MHz with 200000 scans, recycle delay 0.8 s, acquisition time 0.2 s, and processed with a line broadening factor of 30 Hz. The simulated $^{195}Pt\{^1H\}$ NMR spectrum (left, top) was simulated with the coupling constants extracted from the ^{27}Al and $^{31}P\{^1H\}$ NMR spectra using a line width of 470 Hz.

(EFG) at the ^{27}Al site and a long(er) spin lattice relaxation time T_1. Scalar coupling between two spins will only appear if the spin−lattice relaxation times, T_1, of both nuclei are sufficiently long to fulfill the relationship $2\pi JT_1 \gg 1$. If $2\pi JT_1$ for one nucleus, such as aluminum, is long enough, then splitting will be observed for the signal of the other nucleus as shown by Öhmann and Edlund.[50] On the other hand, comparison of the ^{195}Pt satellites in the $^{31}P\{^1H\}$ NMR spectra (measured at 202 MHz) of compound **16** and **17** shows that they are only slightly broader than the central resonance, indicating that the chemical shift anisotropy (CSA) at the ^{195}Pt nuclei seem to be rather small. Furthermore, the relative high magnitude of the coupling constants (ca. 2000 and ca. 3000 Hz) compared with the line width in the ^{195}Pt NMR of about 470 Hz (**16**) leads to the resolved coupling pattern.[51]

The $^{195}Pt\{^1H\}$ NMR spectrum reveals a triplet of sextets at δ = −5550 ($^1J_{Pt-P}$ = 3034 Hz, $^1J_{Pt-Al}$ = 1933 Hz) ppm for compound **16** and a similar coupling pattern at δ = −5410 ($^1J_{Pt-P}$ = 3061 Hz, $^1J_{Pt-Al}$ = 1999 Hz) ppm for compound **17**. The coupling pattern is due to coupling of the ^{195}Pt (I = 1/2) nucleus to the spin 5/2 ^{27}Al nucleus perturbed by additional coupling to the two identical spin 1/2 ^{31}P nuclei. The chemical shift of the respective signal is between that of the bis(phosphine) complex **24** (δ = −6590 ppm) and the typical shift region of *trans*-oxidative addition products (δ = −4780 ppm).[52] As shown in Figure 4 the simulation of the $^{195}Pt\{^1H\}$ NMR spectrum of compound **16** using the NMR spin system analysis module "Daisy" from the NMR Software suite Topspin 3.0 pl4 by Bruker Biospin GmbH shows a triplet of sextets which fits very well to the experiment. However the intensities of the 1:1:1:1:1:1 sextet due to the coupling from the ^{27}Al nucleus are not handled correctly by the software, because of the different T_2 relaxation times of the different spin states of the spin 5/2 nucleus ^{27}Al, which leads to different line widths in the coupling pattern. Normally the outer lines for the ± 5/2 states are smaller in width and higher in intensity than the inner lines corresponding to the ± 1/2 states and the ± 3/2 states exhibit the broadest lines. This behavior is reflected by the experimental $^{195}Pt\{^1H\}$ spectrum in Figure 4, but could not be simulated by the spin system analysis program.

The ^{27}Al NMR spectrum reveals a singlet at δ = 68.5 ppm flanked by ^{195}Pt satellites ($^1J_{Al-Pt}$ = 1933 Hz) for compound **16** and a similar coupling pattern at δ = 44.6 ppm ($^1J_{Al-Pt}$ = 1999 Hz) for compound **17**. Additional ^{27}Al NMR spectra of the PCy_3 analogues **19** and **27** revealed somewhat broader singlets at δ = 67.5 ppm ($^1J_{Al-Pt}$ = 2034 Hz) (**19**) and δ = 41.3 ppm ($^1J_{Al-Pt}$ = 2150 Hz) (**27**). The chemical shifts are in the typical range for AlX_3−Lewis base adducts, while the coupling constants of about 2000 Hz between ^{195}Pt and ^{27}Al proves the connectivity of the Pt−Al unit.[53] Again the relatively sharp and resolved ^{27}Al resonances of compound **16** and **17** indicate that the quadrupolar relaxation plays only a minor role for the ^{27}Al nucleus. Coupling constants for two-bond couplings between ^{27}Al and ^{31}P are typically in the range of 12−30 Hz,[50] but a $^{27}Al-^{31}P$ coupling could not be observed either in the $^{31}P\{^1H\}$ nor in the ^{27}Al NMR spectra of our above-mentioned compounds. For compounds **19** and **27** it was not possible to observe $^{195}Pt\{^1H\}$ NMR signals, probably because of an increased electric field gradient at the ^{27}Al site. Another reason could be the slower tumbling in solution of the larger complex resulting in broader, unresolved NMR lines.

Discussion of Lewis Acid−Base Adducts. Single crystals suitable for X-ray analysis were obtained from a toluene solution at −30 °C (**14** and **16**). The complexes crystallize in space groups $P2_1/n$ (**14**) and $C2/c$ (**16**), respectively (Figure 5). Both compounds feature the characteristic T-shaped geometry at the platinum center observed for complexes of the type $[(Cy_3P)_2Pt-ECl_n]$ (E = Be, Al, Ga, Zr, n = 2, 3, 4) (**13**−**16**) (Figure 5).[30−32] A comparison of the structural data of **16** with **14** reveals (Table 3) very similar Pt−P bond lengths (**14**: 2.287(1) Å; **16**: 2.308(1) and 2.324(1) Å) and P−Pt−P (**16**: 166.42(1)°) and P−Pt−C1 angles (**14**: 165.97(1)°). The

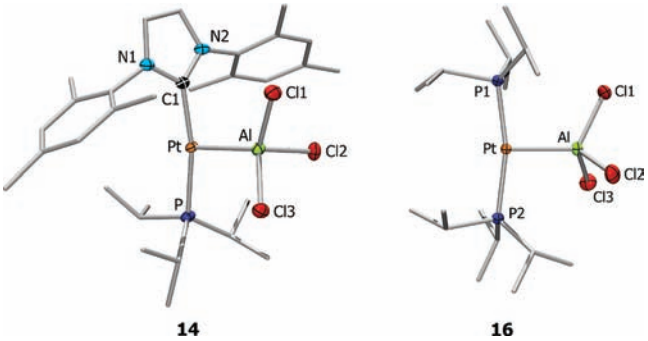

Figure 5. Molecular structures of **14** and **16**. Relevant bond lengths [Å] and angles [deg]: **14**: Pt−Al 2.376(1), Pt−P 2.287(1), Pt−C1 2.009(4), Al−Cl2 2.157(2), Al−Cl1 2.159(2), Al−Cl3 2.169(2); P−Pt−C1 165.97(1), Cl3−Al−Pt 109.92(5), Cl1−Al−Pt 117.72(6), Cl2−Al−Pt 111.84(6), Cl3−Al−Cl1 103.85(6), Cl3−Al−Cl2 107.65(6), Cl1−Al−Cl2 105.16(6); **16**: Pt−Al 2.384(1), Pt−P1 2.308(1), Pt−P2 2.324(1); P1−Pt−P2 166.42(1), Al−Cl1 2.159(1), Al−Cl2 2.152(1), Al−Cl3 2.155(1); P1−Pt−P2 166.42(1), Cl2−Al−Pt 109.85(3), Cl3−Al−Pt 110.48(3), Cl1−Al−Pt 116.75(3), Cl2−Al−Cl3 109.68(3), Cl2−Al−Cl1 104.81(3), Cl3−Al−Cl1 104.95(3). Ellipsoids are drawn at the at the 50% probability level. Ellipsoids of the ligands, solvent molecules, and hydrogen atoms are omitted for clarity.

Pt−Al bond is oriented almost orthogonal to the L−Pt−L′ axis (**14**: C1−Pt−Al 92.90(1)°; P−Pt−Al 101.09(4)°; **16**: P−Pt−Al 96.34(2)° and 97.11(2)°) and the bond lengths are nearly identical (**14**: 2.376(1) Å; **16**: 2.384(1) Å). Additionally, the wider Cl1−Al−Pt angle in compound **16** (Cl1−Al−Pt 116.75(3)°, Cl2−Al−Pt 109.85(3)°, Cl3−Al−Pt 110.48(3)°) is a result of a steric interaction between the chloride and the proximal *i*Pr group. Likewise, in **14** the two wider Cl−Al−Pt angles (Cl1−Al−Pt 117.72(6)°, Cl2−Al−Pt 111.84(6)°, Cl3−Al−Pt 109.92(5)°) can be accounted for by both repulsion between Cl1 and Cl3 and the platinum bound ligands.

As P*i*Pr$_3$ is sterically somewhat less bulky than PCy$_3$, the corresponding base adduct **16** displays a smaller distortion of the overall T-shaped geometry in comparison with [(Cy$_3$P)$_2$Pt−AlCl$_3$] (**19**) as indicated, for example, by comparison of the P1−Pt−P2 angles (**16**: 166.42(1)°, **19**: 162.07(2)°).[31,33]

Discussion of Bis(phosphine) Platinum AlBr$_3$ Adducts. For a structural comparison with our new compound [(*i*Pr$_3$P)$_2$Pt−AlBr$_3$] (**17**) we crystallized compound [(Cy$_3$P)$_2$Pt−AlBr$_3$] (**27**). As mentioned above, we previously employed [(Cy$_3$P)$_2$Pt] (**12**) for the synthesis of MOLPs of the general formula [(Cy$_3$P)$_2$Pt−AlX$_3$] (X = Cl (**19**), Br (**27**), I (**28**)). The AlCl$_3$ adduct was fully characterized by both multinuclear NMR spectroscopy and X-ray structural analysis, whereas the formation of the AlBr$_3$ and AlI$_3$ adducts was indicated by multinuclear NMR spectroscopy only. For compound **27**, the ^{31}P{^{1}H} NMR spectrum shows a singlet at δ = 51.2 ppm flanked by ^{195}Pt satellites ($^1J_{P-Pt}$ = 3046 Hz).[31] Compound **27** could be obtained almost quantitatively as a pale orange solid, but in contrast to the chloro species **19**, readily decomposes in toluene solution within 2−3 days at ambient temperature, forming *trans*-[(Cy$_3$P)$_2$PtBrX] (X = H (**29**), Br (**30**)) (Scheme 2).[54]

Scheme 2. Formation and Decomposition of the Complex [(Cy$_3$P)$_2$Pt−AlBr$_3$] (27).

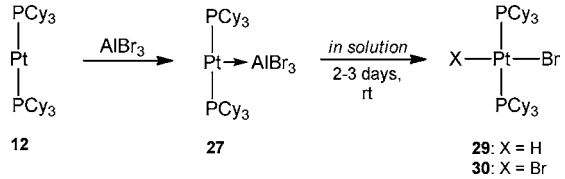

Pale yellow single crystals suitable for X-ray structural analysis were obtained of both **17** and **27** from toluene solutions at −30 °C, thus allowing the first structural comparison between a L$_x$M−ECl$_n$ adduct and its bromo analogue L$_x$M−EBr$_n$. Complex **17** crystallizes in the space group *C*2/*c*, the analogue **27** in the space group $P\bar{1}$, respectively. Both compounds display the expected T-shaped geometry around the platinum center (Figure 6). A comparison of the P$_2$Pt moieties of the chloro species (**19**, **16**) with their respective bromo analogues (**17**, **27**) reveals only minor differences. The Pt−Al distances in compounds **19** and **27** are virtually identical, whereas the Pt−Al distances of **16** (2.384(1) Å) and **17** (2.368(2) Å) differ slightly by 2 pm. DFT calculations on the optimized compounds **16**, **17**, **19**, and **27** showed nearly identical Pt−Al distances (Table 4) and so crystal packing effects could be the reason for the small deviance between theory and experiment. A closer look at the AlBr$_3$ groups of compounds **17** and **27** reveals subtle differences. In compound **17** the torsion angle (P1−Pt−Al−Br1: 0.47(8)°) reveals that the AlBr$_3$ group is eclipsed with respect to the P$_2$Pt moiety. As a result the Al−Br1 bond is elongated (Al−Br1 2.325(2) Å, Al−Br2 2.316(2) Å, Al−Br3 2.313(2) Å) because of a steric interaction between the bromide and a hydrogen atom from the nearby *iso*-propyl group. In compound **27** the conformation is staggered (P1−Pt−Al−Br2: 87.60(4)°) and so the Al−Br distances are similar (Al−Br1 2.319(1) Å, Al−Br2 2.315(1) Å, Al−Br3 2.317 (1) Å).

Comparison of the geometry of the Pt-bound AlBr$_3$ with those of amine-alane adducts derived from computational[55] and experimental studies,[56] suggests that the platinum base exerts a

Table 3. Structural Parameters of Compounds 13−17, 19, 23, 27

	C−Pt[a]	P−Pt[a]	Al−Pt[a]	L−Pt−L[b]
[(Cy$_3$P)$_2$Pt−AlCl$_3$] (**19**)		2.299(1), 2.313(1)	2.386(1)	162.07(2)
[(Cy$_3$P)$_2$Pt−AlBr$_3$] (**27**)		2.303(1), 2.308(1)	2.380(1)	160.09(3)
[(SIMes)(Cy$_3$P)Pt−AlCl$_3$] (**23**)	1.991(9)	2.301(2)	2.384(2)	168.3(5)
[(IMes)(*i*Pr$_3$P)Pt] (**13**)	1.996(2)	2.208(1)		175.71(7)
[(IMes)(*i*Pr$_3$P)Pt−AlCl$_3$] (**14**)	2.009(4)	2.287(1)	2.376(1)	165.97(1)
[(*i*Pr$_3$P)$_2$Pt−AlCl$_3$] (**16**)		2.308(1), 2.324(1)	2.384(1)	166.42(1)
[(*i*Pr$_3$P)$_2$Pt−AlBr$_3$] (**17**)		2.302(2), 2.323(2)	2.368(2)	165.28(5)

[a]Distances in Å. [b]Angles in deg.

dx.doi.org/10.1021/ic300531b | *Inorg. Chem.* 2012, 51, 5617−5626

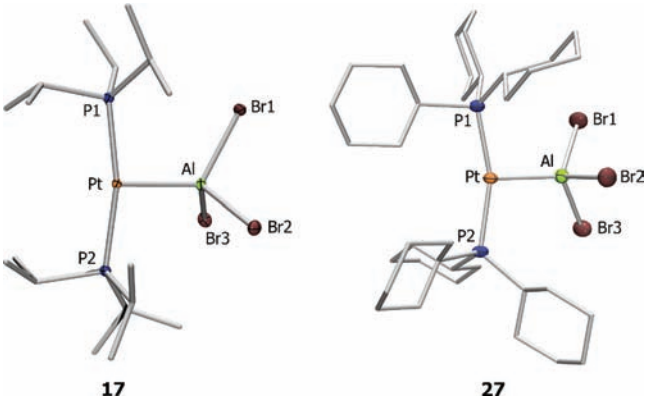

Figure 6. Molecular structure of **17** and **27**. Ellipsoids are drawn at the at the 50% probability level. Ellipsoids of the ligands, solvent molecules and hydrogen atoms are omitted for clarity. Relevant bond lengths [Å] and angles [deg]: **17**: Pt−P1 2.302(2), Pt−P2 2.323(2), Pt−Al 2.368(2), Al−Br1 2.325(2), Al−Br2 2.316(2), Al−Br3 2.325(2); P−Pt−P 165.28(5), Br2−Al−Br3 109.56(7), Br2−Al−Br1 103.74(7), Br3−Al−Br1 103.14(7); **27**: Pt−P1 2.303(1), Pt−P2 2.308(1), Pt−Al 2.380(1), Al−Br1 2.319(1), Al−Br2 2.315(1), Al−Br3 2.317(1); P−Pt−P 160.09(3), Br2−Al−Br3 107.45(4), Br2−Al−Br1 109.09(4), Br3−Al−Br1 99.22(4).

similarly strong electron donation. Thus, the Al−Br distances of **17** (2.313(2)−2.325(2) Å) and **27** (2.3154(11)−2.3193(11) Å) are comparable to that of [tmp−$AlBr_3$] (2.280(2)−2.300(2) Å) (tmp = tetramethylpiperidine) and [H_3N−$AlBr_3$] (2.312 Å mean). The Br−Al−Br angles of **17** (103.14(7)−109.56(7)°) and **27** (99.22(4)°−109.09(4)°) and [tmp−$AlBr_3$] (101.59(7)°−110.02(8)°) are also in a similar range, whereas those of [H_3N−$AlBr_3$] (116.6° mean) are significantly larger.

DFT Calculations. To provide further information as to the Lewis basicity of the different transition metal complexes employed for the synthesis of MOLPs, DFT calculations were carried out (Figure 7). In addition to the optimized structures of [(iPr_3P)$_2$Pt] (**24**), [(IMes)(iPr_3P)Pt] (**13**), and [(SIMes)(iPr_3P)Pt] (**31**), the complexes [(Me_3P)$_2$Pt] (**32**), [(IMe)(Me_3P)Pt] (**33**), and [(SIMe)(Me_3P)Pt] (**34**) were calculated as sterically less-demanding models, as well as their corresponding $AlCl_3$ adducts **35**−**38** (Figure 5) (IMe = *N*,*N*′-bis(methyl)imidazol-2-ylidene, SIMe = *N*,*N*′-bis(methyl)-imidazolylidene).

Interestingly, the saturation of the NHC backbone has no immediate effect on the basicity of the platinum center. Thus, both simplified NHC model complexes **33** and **34** give rise to almost identical BDEs (Table 4) upon adduct formation with $AlCl_3$, which are about 20 kJ/mol more negative than that of **32**. This indicates an increased interaction between the platinum and aluminum centers in NHC complexes, which is in good agreement with previously reported results.[33]

Table 4. Selected Calculated Parameters of [L_2Pt−$AlCl_3$] (14, 16, 34−37) and [L_2Pt] (13, 24, 30−33)

distance	14	16	35	36	37	38
Pt−Al[a]	2.455	2.458	2.459	2.458	2.451	2.451
Pt−L^1[a,b]	2.032	2.362	2.029	2.326	2.041	2.045
Pt−L^2[a]	2.397	2.366	2.405	2.331	2.327	2.333
WBI[c]						
Pt−Al	0.54	0.52	0.54	0.51	0.54	0.54
Pt−L^1[b]	0.56	0.50	0.58	0.51	0.53	0.54
Pt−L^2[b]	0.49	0.50	0.48	0.51	0.53	0.52
natural charge						
Pt	−0.23	−0.31	−0.22	−0.34	−0.25	−0.25
Al	1.31	1.31	1.31	1.31	1.29	1.29
L^1[b]	0.34	0.37	0.33	0.37	0.35	0.33
L^2[b]	0.32	0.36	0.32	0.37	0.35	0.36
L_2Pt	0.43	0.42	0.43	0.40	0.45	0.44
$AlCl_3$	−0.43	−0.42	−0.43	−0.40	−0.45	−0.44
BDE[d]	−131	−146	−130	−167	−188	−189
prep[e] (L^1L^2Pt)[b,d]	48	37	48	13	8	8
prep[e] ($AlCl_3$)[d]	100	96	99	82	86	86
interaction[d]	−279	−278	−277	−262	−282	−282
WBI[c]	13	24	31	32	33	34
WBI[c] Pt−L^1[b]	0.66	0.60	0.68	0.61	0.62	0.64
WBI[c] Pt−L^2[b]	0.61	0.58	0.60	0.61	0.64	0.63
natural charge						
Pt	−0.42	−0.49	−0.41	−0.52	−0.47	−0.46
L^1[b]	0.20	0.25	0.18	0.26	0.23	0.22
L^2[b]	0.22	0.24	0.23	0.26	0.24	0.24

[a]Distances in Å. [b]L^1 = NHC, phosphine; L^2 = phosphine. [c]Wiberg Bond Index. [d]Energies in kJ/mol. [e]Preparation energy, e.g., steric rearrangement during the reaction.

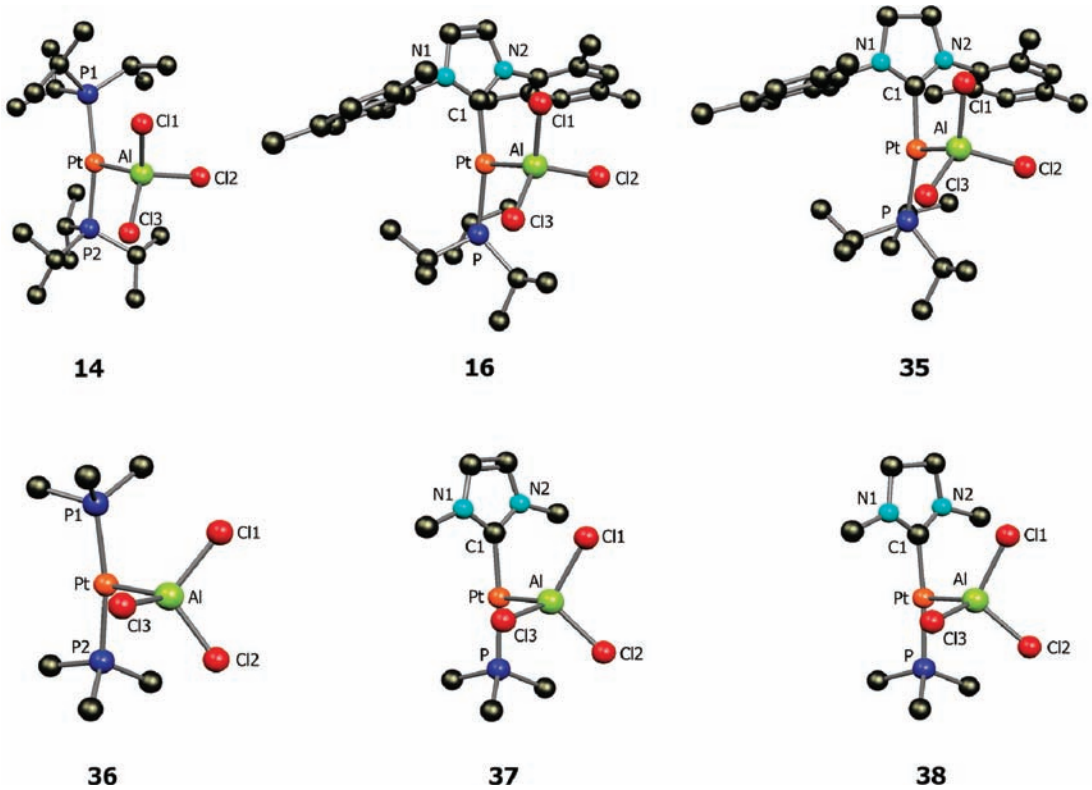

Figure 7. Optimized structures of the compounds **14**, **16**, and **35**−**38**.

However, this trend is reversed in the case of the synthetically employed complexes **13**, **24**, and **31**, which comprise much more sterically demanding phosphine and NHC ligands. Here, the bis(phosphine) complex **13** is determined, by means of the BDE for the Pt−Al bond in the corresponding adduct **16**, to be a stronger transition metal Lewis base than the NHC complexes. The reason for this reversed trend is the significantly increased preparation enthalpy (e.g., the sterical rearrangement of the fragments during adduct formation) in the NHC-containing complexes **13** and **31** (**24**: 37 kJ/mol, **13** and **31**: 48 kJ/mol). Combined with almost identical values for the interaction enthalpies, this leads to an overall less negative BDE for the NHC complexes. Hence, as judged by the interaction energies alone, P*i*Pr$_3$ appears to exert the same electronic influence on the platinum center as the NHCs IMes and SIMes. This finding is in stark contrast to earlier calculations on corresponding PCy$_3$ complexes. Here, the bis(phosphine) complex [(Cy$_3$P)$_2$Pt−AlCl$_3$] (**19**) revealed a significantly reduced interaction enthalpy (ca. 20 kJ/mol) in comparison to the mixed-ligand complexes with PCy$_3$ and NHC I^{t}Bu ligands (I^{t}Bu = *N*,*N*′-bis(*tert*-butyl)imidazol-2-ylidene).[33] Analysis of the natural charges, as calculated by the natural bond orbital (NBO) method, reveals a uniform trend for all investigated systems, both the models **36**−**38** and the authentic complexes **14**, **16**, and **35**. Upon adduct formation, the overall natural charge of the neutral L$_2$Pt fragment (by definition natural charge = 0) in all compounds is increased to about 0.41−0.45, because of electron donation from the metal atom to the Lewis acid AlCl$_3$. This positive charge is distributed between the platinum center and the ligands, respectively. For example in complex **14**, the natural charge of the IMes ligand is increased by 0.14 (0.20 in **13** to 0.34 in **14**), whereas an almost identical increase is found for the P*i*Pr$_3$ ligand (0.22 in **13** to 0.32 in **14**). Therefore, again similar electronic properties for IMes and P*i*Pr$_3$ are found. In addition to the decreased negative charge of the platinum atom (−0.42 in **13** to −0.22 in **14**) this sums up to an overall positive charge of 0.44 for the [(IMes)(*i*PrP$_3$)Pt] fragment in the MOLP **14** (Table 4).

In further calculations, the influence of the halogen atoms on the properties of the MOLPs [(Cy$_3$P)$_2$Pt−AlX$_3$] (X = Cl (**19**), Br (**27**), and I (**28**)) and [(*i*Pr$_3$P)$_2$Pt−AlX$_3$] (X = Cl (**16**), Br (**17**)) was investigated.[31] Here, a clear trend was observed, that is, the Pt−Al BDE decreases as the group is descended (Table 5). The strongest interaction was found for the AlCl$_3$ adduct (**19**: BDE = −141 kJ/mol, **16**: BDE = −146 kJ/mol), followed by the AlBr$_3$ (**27**: BDE = −124 kJ/mol, **17**: BDE = −126 kJ/mol) and the AlI$_3$ species (**28**, BDE = −106 kJ/mol). A

Table 5. Selected Calculated Parameters of [(Cy$_3$P)$_2$Pt−AlX$_3$] and [(*i*Pr$_3$P)$_2$Pt−AlX$_3$]

	19	27	28	16	17
X	Cl	Br	I	Cl	Br
Pt−Al[a]	2.459	2.462	2.461	2.458	2.459
WBI[b] Pt−Al	0.52	0.54	0.55	0.52	0.53
WBI[b] Pt−P	0.5	0.49	0.48	0.50	0.49
natural charge					
Pt	−0.31	−0.29	−0.26	−0.31	−0.29
Al	1.31	1.1	0.67	1.31	1.09
BDE[c]	−141	−124	−106	−146	−129
prep[d] [L$_2$Pt][c]	40	45	51	37	42
prep[d] (AlX$_3$)[c]	98	100	98	96	98
interaction[c]	−279	−269	−256	−278	−269

[a]Distances in Å. [b]Wiberg Bond Index. [c]Energies in kJ/mol. [d]Preparation energy, e.g., steric rearrangement during the reaction.

dx.doi.org/10.1021/ic300531b | *Inorg. Chem.* 2012, 51, 5617−5626

possible explanation for this trend is the reduced electrostatic interaction in the adducts with less electronegative halogens. The disparity between the natural charges of platinum and aluminum is most distinct in **19** and **16** (1.6) and is reduced when the chlorine is substituted by bromine (**27** and **17**: 1.4) or iodine (**28**: 0.9). Furthermore, the preparation enthalpy of $[(Cy_3P)_2Pt]$ (**12**) upon adduct formation is more positive for heavier halogens. As expected, AlI_3 is the weakest Lewis acid with respect to MOLP formation in the investigated systems (Table 5). This result supports the earlier reports by Frenking et al. for group 10 complexes of the type $[(Me_3P)_2Pt{-}EX_3]$ (E = B, Al; X = Cl, Br, I).[26]

■ CONCLUSION

Herein, we report on the synthesis of the new heteroleptic NHC-phosphine complex $[(IMes)(iPr_3P)Pt]$ (**13**) and its characterization by multinuclear NMR spectroscopy, elemental analysis, and single crystal X-ray diffraction analysis. Additionally, the alane adducts of **13** and the homoleptic Pt(0) compound $[(iPr_3P)_2Pt]$ (**24**) were prepared and fully characterized (**14**−**17**) including multinuclear NMR, structural, and computational data. For compounds **16** and **17** both ^{27}Al NMR and ^{195}Pt NMR spectra were obtained, both of which displayed the $^1J(^{27}Al{-}^{195}Pt)$ spin−spin coupling—to the best of our knowledge this is the first time this coupling has been observed. According to computational analysis, the $PiPr_3$ ligand seems to exert a similar electronic influence on the platinum centers as the investigated NHCs, that is, IMes and SIMes. This finding contrasts previous studies on PCy_3 complexes, in which the phosphine appeared to be a weaker electron donor than NHC ligands. In the course of our theoretical investigations, we further examined the MOLPs $[(Cy_3P)_2Pt{-}AlBr_3]$ (**27**) and $[(Cy_3P)_2Pt{-}AlI_3]$ (**28**). Here, the expected trend for the decrease of the Lewis acidity of the alanes with increase of the atomic number of the halogen atoms was confirmed.

■ EXPERIMENTAL SECTION

General Considerations. All manipulations were performed in an inert atmosphere of argon using standard Schlenk and glovebox techniques. Solvents were distilled over alkali metal, degassed, and stored over molecular sieves (4 Å) under argon. Deuterated solvents were degassed by three freeze−pump−thaw cycles and stored under argon over molecular sieves. NMR experiments were performed on a Bruker Avance 500 (^1H: 500.1 MHz; ^{13}C: 125.8 MHz; ^{27}Al: 130.3 MHz; ^{31}P: 202.5 MHz; ^{195}Pt: 107.5 MHz) apparatus. ^1H NMR and $^{13}C\{^1H\}$ NMR spectra were calibrated to TMS; in the case of ^{27}Al NMR spectra $Al(NO_3)_3$ in D_2O was used as external standard, and for $^{31}P\{^1H\}$ NMR spectra 85% H_3PO_4 was used. The external standard for the $^{195}Pt\{^1H\}$ NMR spectra was $Na_2[PtCl_6]$ in D_2O. Elemental analyses were performed on an Elementar vario Micro Cube elemental analyzer and Leco Instrumente CHNS 932 elemental analyzer. $[(Cy_3P)_2Pt]$,[47] $[(iPr_3P)_3Pt]$[47] and IMes[57] were prepared according to known methods.

[(IMes)(iPr$_3$P)Pt] (**13**). IMes (19 mg, 58 μmol) and $[(iPr_3P)_3Pt]$ (**25**) (40 mg, 58 μmol) were dissolved in hexane (1.0 mL). The intensely yellow solution was kept at −30 °C for 5 d and yellow crystals were obtained after 3 days (29 mg, 44 μmol, 70%). ^1H NMR (500.1 MHz, C_6D_6): δ = 6.84−6.83 (m, 4H, *m*-H_{ar}), 6.21 (d, $^3J_{H-H}$ = 1 Hz, 2H, NC*H*C*H*N), 2.37 (s, 12H, *o*-CH_3, Mes), 2.17 (s, 6H, *p*-CH_3, Mes), 1.74−1.65 (m, 3H, C*H*, *i*Pr), 1.09−1.07 (m, 18H, CH_3, *i*Pr) ppm. $^{13}C\{^1H\}$ NMR (125.8 MHz, C_6D_6): δ = 201.5 (s, NCN), 138.3 (s, *ipso*-C_{ar}), 137.4 (s, *p*-C_{ar}), 135.6 (s, *o*-C_{ar}), 128.8 (s, *m*-C_{ar}), 119.2 (s, NCHCHN), 25.6 (d, $^1J_{C-P}$ = 24 Hz, CH, *i*Pr), 21.3 (d, $^2J_{C-P}$ = 11 Hz; CH_3, *i*Pr), 21.2 (s, *p*-CH_3, Mes), 18.8 ppm (s, *o*-CH_3, Mes) ppm. $^{31}P\{^1H\}$ NMR (202.5 MHz, C_6D_6): δ = 69.4 ($^1J_{P-Pt}$ = 3897 Hz) ppm. $^{195}Pt\{^1H\}$ NMR (107.5 MHz, C_6D_6): δ = −6290 ($^1J_{Pt-P}$ = 3897 Hz) ppm. Elemental analysis (%) calculated for $C_{30}H_{46}N_2PPt$: C 54.53, H 7.02, N 4.24; found: C 53.89, H 6.67, N 4.06.

[(IMes)(iPr$_3$P)Pt(AlCl$_3$)] (**14**). $AlCl_3$ (2.0 mg, 15 μmol) and $[(IMes)(iPr_3P)Pt]$ (**13**) (10 mg, 15 μmol) were dissolved in benzene (1.0 mL) at ambient temperature. A yellow solid precipitated immediately, was filtered off and rinsed with benzene. The precipitate was dissolved in toluene and yellow crystals were obtained after 24 h at −30 °C (7 mg, 10 μmol, 65%). ^1H NMR (500.1 MHz, C_6D_6): δ = 6.81 (m, 4H, H_{ar}), 6.13 (d, 2H, $^3J_{H-H}$ = 1 Hz, NC*H*C*H*N), 2.34 (s, 12H, *o*-CH_3, Mes), 2.14 (s, 6H, *m*-CH_3, Mes), 1.30−1.20 (m, 3H, C*H*, *i*Pr), 1.02−0.98 (m, 18H, CH_3, *i*Pr) ppm. $^{13}C\{^1H\}$ NMR (125.8 MHz, C_6D_6): δ = 179.7 (s, NCN), 135.4 (s, *ipso*-C_{ar}), 134.4 (s, *p*-C_{ar}), 129.7 (s, *o*-C_{ar}), 128.3 (s, *m*-C_{ar}), 122.9 (s, NCHCHN), 25.1 (d, $^1J_{C-P}$ = 25 Hz, CH, *i*Pr), 20.0 (s, *p*-CH_3, Mes), 19.9 (s, CH_3, *i*Pr), 17.7 (s, *o*-CH_3, Mes) ppm. ^{27}Al NMR (130.3 MHz, C_6D_6): δ = 68.9 ($^1J_{Al-Pt}$ = 2100 Hz) ppm. $^{31}P\{^1H\}$ NMR (202.5 MHz, C_6D_6): δ = 56.9 ($^1J_{P-Pt}$ = 2988 Hz) ppm. Elemental analysis (%) calculated for $C_{37}H_{50}AlCl_3N_2PPt$: C 50.37; H 5.71; N 3.18; found: C 50.11; H 5.72; N 3.51.

[(IMes)(iPr$_3$P)Pt(AlBr$_3$)] (**15**). $AlBr_3$ (8.0 mg, 30 μmol) was added to a solution of $[(IMes)(iPr_3P)Pt]$ (**13**) (20 mg, 30 μmol) in toluene (1.0 mL) at −30 °C. A yellow solid precipitated after 48 h, which was filtered off and rinsed with toluene. The precipitate was dissolved in toluene and yellow crystals were obtained after 24 h at −30 °C (19 mg, 21 μmol, 71%). ^1H NMR (500.1 MHz, C_6D_6): δ = 6.74 (s, 4H, H_{ar}), 6.26 (s, 2H, NC*H*C*H*N), 2.29 (s, 12H, *o*-CH_3, Mes), 2.10 (s, 6H, *m*-CH_3, Mes), 1.80−1.69 (m, 3H, C*H*, *i*Pr), 0.89−0.81 (m, 18H, CH_3, *i*Pr) ppm. $^{13}C\{^1H\}$ NMR (125.8 MHz, C_6D_6): δ = 167.9 (s, NCN), 138.4 (s, *ipso*-C_{ar}), 136.6 (s, *p*-C_{ar}), 136.0 (s, *o*-C_{ar}), 129.5 (s, *m*-C_{ar}), 122.9 (s, NCHCHN), 25.6 (d, $^1J_{C-P}$ = 25 Hz, CH, *i*Pr), 20.9 (s, *p*-CH_3, Mes), 19.6 (s, CH_3, *i*Pr), 19.2 ppm (s, *o*-CH_3, Mes) ppm. ^{27}Al NMR (130.3 MHz, C_6D_6): δ = 42.7 ($^1J_{Al-Pt}$ = 2200 Hz) ppm. $^{31}P\{^1H\}$ NMR (202.5 MHz, C_6D_6): δ = 53.5 ($^1J_{P-Pt}$ = 2980 Hz) ppm. Elemental analysis (%) calculated for $C_{37}H_{50}AlCl_3N_2PPt$: C 38.89; H 4.90; N 3.02; found: C 38.92; H 4.85; N 3.06.

[(iPr$_3$P)$_2$Pt(AlCl$_3$)] (**16**). In a J. Young NMR tube $AlCl_3$ (4.0 mg, 30 μmol) was added to a yellow solution of $[(iPr_3P)_2Pt]$ (**24**) (20 mg, 30 μmol) in benzene (0.6 mL). The color of the reaction mixture lightened, and a yellow solid precipitated. The precipitate was filtered off and rinsed with hexane. For X-ray analysis suitable crystals were obtained from a solution in benzene at ambient temperature after 24 h (13 mg, 20 μmol, 67%). ^1H NMR (500.1 MHz, C_6D_6): δ = 2.48−2.40 (sep, $^3J_{H-H}$ = 4 Hz, 6H, C*H*), 1.23−1.08 (q, $^3J_{H-H}$ = 8 Hz, 36H, CH_3) ppm. $^{13}C\{^1H\}$ NMR (125.8 MHz, C_6D_6): δ = 26.0 (vt, $N = |^1J_{C-P}+{}^3J_{C-P}|$ = 25 Hz, CH, *i*Pr), 20.9 (s, CH_3, *i*Pr) ppm.[58] ^{27}Al NMR (130.3 MHz, C_6D_6): δ = 68.5 ($^1J_{Al-Pt}$ = 1933 Hz) ppm. $^{31}P\{^1H\}$ NMR (202.5 MHz, C_6D_6): δ = 65.5 ($^1J_{P-Pt}$ = 3034 Hz) ppm. $^{195}Pt\{^1H\}$ NMR (107.5 MHz, C_6D_6): δ = −5550 ($^1J_{Pt-P}$ = 3034 Hz, $^1J_{Pt-Al}$ = 1933 Hz) ppm. Elemental analysis (%) calculated for $C_{18}H_{42}AlCl_3P_2Pt$: C 33.32; H 6.52; found: C 33.38; H 6.61.

[(iPr$_3$P)$_2$Pt(AlBr$_3$)] (**17**). In a J. Young NMR tube $AlBr_3$ (14 mg, 52 μmol) was added to a yellow solution of $[(iPr_3P)_2Pt]$ (**24**) (35 mg, 52 μmol) in benzene (0.7 mL) at 0 °C. The color of the reaction mixture deepened and a yellow solid precipitated. The precipitate was filtered off and rinsed with hexane. For X-ray analysis suitable crystals were obtained from a solution in benzene at ambient temperature after 24 h (15 mg, 20 μmol, 52%). ^1H NMR (500.1 MHz, C_6D_6): δ = 2.67−2.58 (sep, $^3J_{H-H}$ = 4 Hz, 6H, C*H*), 1.19−1.14 (q, $^3J_{H-H}$ = 8 Hz, 36H, CH_3) ppm. $^{13}C\{^1H\}$ NMR (125.8 MHz, C_6D_6): δ = 25.9 (vt, $N = |^1J_{C-P}+{}^3J_{C-P}|$ = 25 Hz, CH, *i*Pr), 20.9 (s, CH_3, *i*Pr) ppm.[58] ^{27}Al NMR (130.3 MHz, C_6D_6): δ = 44.6 ($^1J_{Al-Pt}$ = 1999 Hz) ppm. $^{31}P\{^1H\}$ NMR (202.5 MHz, C_6D_6): δ = 63.1 ($^1J_{P-Pt}$ = 3061 Hz) ppm. $^{195}Pt\{^1H\}$ NMR (107.5 MHz, C_6D_6): δ = −5410 ($^1J_{Pt-P}$ = 3061 Hz, $^1J_{Pt-Al}$ = 1999 Hz) ppm. Elemental analysis (%) calculated for $C_{18}H_{42}AlBr_3P_2Pt$: C 27.64; H 5.41; found: C 26.95; H 5.26.

[(Cy$_3$P)$_2$Pt(AlBr$_3$)] (**27**). $AlBr_3$ (8.0 mg, 29 μmol) was added to a pale yellow solution of $[(Cy_3P)_2Pt]$ (**12**) (21 mg, 28 μmol) in toluene (0.6 mL). The solvent from the orange solution was removed in vacuo to obtain **27** (28 mg, 27 μmol, 98%) as a light orange solid. Suitable crystals were obtained by means of diffusion of hexane to a toluene

solution at −30 °C. ^{1}H NMR (500.1 MHz, d_8-tol): δ = 2.69−2.65 (m, 6H, Cy), 2.22−1.03 ppm (m, 60H, Cy). ^{13}C{^{1}H} NMR (125.8 MHz, d_8-tol): δ = 36.3 (vt, $N = |^1J_{C-P}+{}^3J_{C-P}|$ = 25 Hz, C^1, Cy), 31.6 (s, C^3, C^5, Cy), 27.9 (vt, $N = |^2J_{P-C}+{}^4J_{P-C}|$ = 11 Hz, C^2, C^6, Cy), 26.6 ppm (s, C^4, Cy).[58] ^{27}Al NMR (130.3 MHz, d_8-tol): δ = 41.3 ($^1J_{Al-Pt}$ = 2150 Hz) ppm. ^{31}P{^{1}H} NMR (202.5 MHz, d_8-tol): δ = 51.2 ppm ($^1J_{P-Pt}$ = 3046 Hz). Elemental analysis (%) calculated for $C_{36}H_{66}AlBr_3P_2Pt$: C 42.28, H 6.50; found: C 42.74, H 6.77.

Crystal Structure Determination. The crystal data of **13**, **14**, **16**, and **27** were collected on a Bruker Apex diffractometer with a CCD area detector and graphite monochromated $Mo_{K\alpha}$ radiation. The structures were solved using direct methods, refined with the Shelx software package and expanded using Fourier techniques.[59] All non-hydrogen atoms were refined anisotropically. Hydrogen atoms were assigned to idealized positions and were included in structure factor calculations.

Crystal Data for ***13***. $C_{30}H_{45}N_2PPt$, M_r = 659.74, yellow block, 0.31 × 0.16 × 0.06 mm^3, triclinic space group $P\bar{1}$, a = 10.3236(18) Å, b = 10.8091(18) Å, c = 15.026(3) Å, α = 78.494(4)°, β = 77.506(4)°, γ = 66.744(3)°, V = 1491.8(4) Å^3, Z = 2, ρ_{calcd} = 1.469 g·cm^{-3}, μ = 4.776 mm^{-1}, F(000) = 664, T = 173(2) K, R_1 = 0.0203, wR^2 = 0.0492, 5858 independent reflections [$2\theta \leq 52.06°$] and 319 parameters.

Crystal Data for ***14***. $C_{37}H_{50}AlCl_3N_2PPt$, M_r = 882.18, yellow block, 0.37 × 0.16 × 0.15 mm^3, monoclinic space group $P2_1/n$, a = 10.7618(3) Å, b = 16.4437(4) Å, c = 22.3018(5) Å, β = 100.4370(10)°, V = 3881.31(17) Å^3, Z = 4, ρ_{calcd} = 1.510 g·cm^{-3}, μ = 3.913 mm^{-1}, F(000) = 1772, T = 100(2) K, R_1 = 0.0288, wR^2 = 0.0664, 7949 independent reflections [$2\theta \leq 52.78°$] and 483 parameters.

Crystal Data for ***16***. $C_{18}H_{42}AlCl_3P_2Pt$, M_r = 648.88, yellow block, 0.22 × 0.17 × 0.085 mm^3, monoclinic space group $C2/c$, a = 31.069(8) Å, b = 10.862(3) Å, c = 17.407(5) Å, β = 118.672(3)°, V = 5154(2) Å^3, Z = 8, ρ_{calcd} = 1.672 g·cm^{-3}, μ = 5.916 mm^{-1}, F(000) = 2576, T = 173(2) K, R_1 = 0.0172, wR^2 = 0.0375, 6442 independent reflections [$2\theta \leq 56.74°$] and 238 parameters.

Crystal Data for ***17***. $C_{18}H_{42}AlBr_3P_2Pt$, M_r = 782.26, yellow block, 0.29 × 0.15 × 0.08 mm^3, Monoclinic space group $C2/c$, a = 31.4522(17) Å, b = 10.9575(5) Å, c = 17.4716(9) Å, β = 118.731(3)°, V = 5280.1(5) Å^3, Z = 8, ρ_{calcd} = 1.968 g·cm^{-3}, μ = 10.012 mm^{-1}, F(000) = 3008, T = 100(2) K, R_1 = 0.0525, wR^2 = 0.1121, 9534 independent reflections [$2\theta \leq 53.92°$] and 239 parameters.

Crystal Data for ***27***. $C_{93}H_{156}Al_2Br_6P_4Pt_2$, M_r = 2321.58, yellow plate, 0.49 × 0.025 × 0.021 mm^3, triclinic space group $P\bar{1}$, a = 9.8756(11) Å, b = 11.2140(12) Å, c = 22.450(2) Å, α = 96.912(2)°, β = 93.273(2)°, γ = 94.380(2)°, V = 2455.4(5) Å^3, Z = 1, ρ_{calcd} = 1.570 g·cm^{-3}, μ = 5.411 mm^{-1}, F(000) = 1166, T = 173(2) K, R_1 = 0.0281, wR^2 = 0.0674, 9757 independent reflections [$2\theta \leq 52.4°$] and 445 parameters.

Crystallographic data have been deposited with the Cambridge Crystallographic Data Center as supplementary publication no. CCDC-854859 (**13**), CCDC-854860 (**14**), CCDC-854861 (**16**), CCDC-868866 (**17**), and CCDC-854862 (**27**). These data can be obtained free of charge from the Cambridge Crystallographic Data Centre via www.ccdc.cam.ac.uk/data_request/cif.

■ ASSOCIATED CONTENT

Supporting Information

Cartesian coordinates of all optimized geometries as well as CIF files giving crystallographic data of **13**, **14**, **16**, **17**, and **27**. This material is available free of charge via the Internet at http://pubs.acs.org.

■ AUTHOR INFORMATION

Corresponding Author

*E-mail: h.braunschweig@mail.uni-wuerzburg.de. Fax: +49-(0)931/31-85263. Phone: +49-(0)931/31-85260.

Notes

The authors declare no competing financial interest.

■ ACKNOWLEDGMENTS

We are grateful to the German Science Foundation (DFG) for financial support. J.B. is grateful to the Fonds der Chemischen Industrie for a doctoral scholarship.

■ REFERENCES

(1) Vaska, L.; DiLuzio, J. W. *J. Am. Chem. Soc.* **1961**, *83*, 2784−2785.
(2) Baird, M. C.; Wilkinson, G. *Chem. Commun.* **1966**, 267−268.
(3) Vaska, L.; DiLuzio, J. W. *J. Am. Chem. Soc.* **1962**, *84*, 679−680.
(4) Shriver, D. F. *J. Am. Chem. Soc.* **1963**, *85*, 3509−3510.
(5) Braunschweig, H.; Wagner, T. *Chem. Ber.* **1994**, *127*, 1613−1614.
(6) Werner, H. *Pure Appl. Chem.* **1982**, *54*, 177−188.
(7) Werner, H. *Angew. Chem.* **1983**, *95*, 932−954; *Angew. Chem., Int. Ed.* **1983**, *22*, 927−949.
(8) Werner, H.; Dey, K. *Chem. Ber.* **1979**, *112*, 823−833.
(9) Mayer, J. M.; Calabrese, J. C. *Organometallics* **1984**, *3*, 1292−1298.
(10) Golden, J. T.; Peterson, T. H.; Holland, P. L.; Bergmann, R. G.; Andersen, R. A. *J. Am. Chem. Soc.* **1998**, *120*, 223−224.
(11) Amati, M.; Lelj, F. *Can. J. Chem.* **2009**, *87*, 1406−1414.
(12) Steinke, T.; Fischer, R. A.; Winter, M.; Cokoja, M.; Gemel, C. *Dalton Trans.* **2005**, 55−62.
(13) Braunschweig, H.; Dewhurst, R. D.; Schneider, A. *Chem. Rev.* **2010**, *110*, 3924−3957.
(14) Dang, L.; Zhenyang, L.; Marder, T. B. *Chem. Commun.* **2009**, 3987−3995.
(15) Burgess, K.; Ohlmeyer, M. J. *Chem. Rev.* **1991**, *91*, 1179−1191.
(16) Marder, T. B.; Norman, N. C. *Top. Catal.* **1998**, *5*, 63−73.
(17) Thomas, R. L.; Souza, F. E.; Marder, T. B. *J. Chem. Soc., Dalton Trans.* **2001**, 1650−1656.
(18) Braunschweig, H.; Radacki, K.; Schneider, A. *Science* **2010**, *328*, 345−347.
(19) Clegg, W.; Lawlor, F. J.; Lesley, G.; Marder, T. B.; Norman, N. C.; Orpen, A. G.; Quayle, M. J.; Rice, C. R.; Scott, A. J.; Souza, F. E. *J. Organomet. Chem.* **1998**, *550*, 183−192.
(20) Bauer, J.; Braunschweig, H.; Kraft, K.; Radacki, K. *Angew. Chem., Int. Ed.* **2011**, *50*, 10457−10460.
(21) Arnold, N.; Braunschweig, H.; Brenner, P.; Jimenez-Halla, J. O.; Kupfer, T.; Radacki, K. *Organometallics* **2012**, *31*, 1897−1907.
(22) Braunschweig, H.; Brenner, P.; Müller, A.; Radacki, K.; Rais, D.; Uttinger, K. *Chem.—Eur. J.* **2007**, *13*, 7171−7176.
(23) Braunschweig, H.; Radacki, K.; Uttinger, K. *Inorg. Chem.* **2007**, *46*, 8796−8800.
(24) Zeng, G.; Sakaki, S. *Inorg. Chem.* **2011**, *50*, 5290−5297.
(25) Braunschweig, H.; Gruss, K.; Radacki, K. *Inorg. Chem.* **2008**, *47*, 8595−8597.
(26) Goedecke, C.; Hillebrecht, P.; Uhlemann, T.; Haunschild, R.; Frenking, G. *Can. J. Chem.* **2009**, *87*, 1470−1479.
(27) Plumley, J. A.; Evanseck, J. D. *J. Phys. Chem. A* **2009**, *113*, 5985−5992.
(28) Mandal, S. K.; Roesky, H. W. *Advances in Catalysis*, 54th ed; Academic Press: London, U.K., 2011; pp 1−61.
(29) Corma, A.; Garcia, H. *Chem. Rev.* **2003**, *103*, 4307−4366.
(30) Braunschweig, H.; Gruss, K.; Radacki, K. *Angew. Chem.* **2009**, *121*, 4303−4305; *Angew. Chem., Int. Ed.* **2009**, *48*, 4239−4241.
(31) Braunschweig, H.; Gruss, K.; Radacki, K. *Angew. Chem.* **2007**, *119*, 7929−7931; *Angew. Chem., Int. Ed.* **2007**, *46*, 7782−7784.
(32) Braunschweig, H.; Radacki, K.; Schwab, K. *Chem. Commun.* **2010**, *46*, 913−915.
(33) Bauer, J.; Braunschweig, H.; Brenner, P.; Kraft, K.; Radacki, K.; Schwab, K. *Chem.—Eur. J.* **2010**, *16*, 11985−11992.
(34) Poater, A.; Cosenza, B.; Correa, A.; Giudice, S.; Ragone, F.; Scarano, V.; L. Cavallo, L. *Eur. J. Inorg. Chem.* **2009**, *32*, 1759−1766.
(35) Ragone, F.; Poater, A.; Cavallo, L. *J. Am. Chem. Soc.* **2010**, *132*, 4249−4258.
(36) Tolman, C. A. *Chem. Rev.* **1977**, *77*, 314−348.
(37) Chianese, A. R.; Li, X.; Janzen, M. C.; Faller, J. W.; Crabtree, R. H. *Organometallics* **2003**, *22*, 1663−1667.

(38) Kelly, R. A., III; Clavier, H.; Giudice, S.; Scott, N. M.; Stevens, E. D.; Bordner, J.; Samardjiev, I.; Hoff, C. D.; Cavallo, L.; Nolan, S. P. *Organometallics* **2008**, *27*, 202−210.
(39) Ros, R.; Tassan, A.; Laurenczy, G.; Roulet, R. *Inorg. Chim. Acta* **2000**, *303*, 94−99.
(40) Braunschweig, H.; Radacki, K.; Rais, D.; Uttinger, K. *Angew. Chem.* **2006**, *118*, 169; *Angew. Chem., Int. Ed.* **2006**, *45*, 162−165.
(41) Braunschweig, H.; Kupfer, T.; Radacki, K.; Schneider, A.; Seeler, F.; Uttinger, K.; Wu, H. *J. Am. Chem. Soc.* **2008**, *130*, 7974−7983.
(42) Fu, G. C.; Nguyen, S. T.; Grubbs, R. H. *J. Am. Chem. Soc.* **1993**, *115*, 9858−9859.
(43) Scholl, M.; Ding, S.; Lee, C. W.; Grubbs, R. H. *Org. Lett.* **1999**, *1*, 953−956.
(44) Sanford, M. S.; Love, J. A.; Grubbs, R. H. *J. Am. Chem. Soc.* **2001**, *123*, 6543−6554.
(45) Scott, N. M.; Nolan, S. P. *Eur. J. Inorg. Chem.* **2005**, *10*, 1815−1828.
(46) Clavier, H.; Nolan, S. P. *Chem. Commun.* **2010**, *46*, 841−861.
(47) Yoshida, T.; Otsuka, S. *Inorg. Synth* **1990**, *28*, 113−126.
(48) Otsuka, S. *J. Organomet. Chem.* **1980**, *200*, 191−205.
(49) Arduengo, A. J., III; Gamper, S. F.; Calabrese, J. C.; Davidson, F. *J. Am. Chem. Soc.* **1994**, *116*, 4391−4394.
(50) Öhman, L.-O..; Edlund, U. Aluminium-27 NMR of solids. In *Encyclopedia of NMR*; Grant, D. M., Harris, R. K., Eds.; John Wiley & Sons: Chichester, U.K., 1996; Vol. *2*, pp 742−750.
(51) Rehder, D. *Chimia* **1986**, *40*, 186−199.
(52) Pregosin, P. S. Group 10 Nickel to Platinum. In *Transition Metal NMR*; Elsevier: München, Germany, 1991; Vol. *13*, pp 217−263.
(53) Vriezen, W. H.; Jellinek, F. *Chem. Phys. Lett.* **1967**, *1*, 284.
(54) (a) Jasim, N. A.; Perutz, R. N. *J. Am. Chem. Soc.* **2000**, *122*, 8685−8693. (b) Cameron, T. S.; Clark, H. C.; Linden, A.; Nicholas, A. M. *Polyhedron* **1990**, *9*, 1683−1688.
(55) Timoshkin, A.; Suvorov, A.; Bettinger, H. F.; Schaefer, H. F. *J. Am. Chem. Soc.* **1999**, *121*, 5687−5699.
(56) Krossing, I.; Nöth, H.; Schwenk-Kirchner, H.; Seifert, T.; Tacke, C. *Eur. J. Inorg. Chem.* **1998**, *12*, 1925−1930.
(57) (a) Arduengo III, A. J. U.S. Patent 5 077 414, 1991; (b) Arduengo, A. J., III; Bock, H.; Chen, H.; Denk, M.; Dixon, D. A.; Green, J. C.; Herrman, W. A.; Jones, N. L.; Wagner, M.; West, R. *J. Am. Chem. Soc.* **1994**, *116*, 6641−6649.
(58) Fackler, J. P., Jr.; Fetchin, J. A.; Mayhew, J.; Seidel, W. C.; Swift, T. J.; Weeks, M. *J. Am. Chem. Soc.* **1969**, *91*, 1941−1947.
(59) Sheldrick, G. M. *Acta Crystallogr.* **2008**, *A64*, 112−122.